

PREPARED FOR SUBMISSION TO JHEP

# Testing the Higgs Boson Coupling to Gluons

---

U. Langenegger,<sup>a</sup> M. Spira,<sup>a</sup> I. Strebel<sup>a,b</sup>

<sup>a</sup>*Paul Scherrer Institute, CH-5232 Villigen PSI, Switzerland*

<sup>b</sup>*ETH Zurich, CH-8093 Zurich, Switzerland*

*E-mail:* [urs.langenegger@psi.ch](mailto:urs.langenegger@psi.ch), [michael.spira@psi.ch](mailto:michael.spira@psi.ch),  
[strebeli@phys.ethz.ch](mailto:strebeli@phys.ethz.ch)

ABSTRACT: We study the possibility to separate in gluon fusion loop-induced Higgs boson production from point-like production. The Higgs boson is reconstructed in the  $H \rightarrow \gamma\gamma$  final state at very large transverse momentum. Using the Higgs boson yields (normalized to the overall rate) and the shape of the Higgs boson  $p_{\perp}$  distribution the two hypotheses can be separated with 2 standard deviations with an integrated luminosity of about  $500 \text{ fb}^{-1}$ . The largest experimental uncertainty affecting this estimate is the background event yield. The theoretical uncertainties from missing top mass effects are large, but can be decreased with dedicated calculations.

---

## Contents

<b>1</b>	<b>Introduction</b>	<b>1</b>
<b>2</b>	<b>Simulation setup</b>	<b>3</b>
<b>3</b>	<b>Analysis</b>	<b>5</b>
3.1	Event Reconstruction	5
3.2	Sensitivity Analysis	7
<b>4</b>	<b>Results</b>	<b>7</b>
<b>5</b>	<b>Conclusions</b>	<b>9</b>
<b>6</b>	<b>Acknowledgements</b>	<b>10</b>

---

## 1 Introduction

Since the discovery of a Higgs-like state at the LHC [1] huge efforts have been made to study its properties in detail [2] in order to test consistency with the predictions of a Standard Model (SM) Higgs particle [3]. Its couplings to vector bosons and fermions agree with SM expectations within errors. The present state of the analyses at the LHC underline the  $\mathcal{CP}$ -even and spinless nature of the discovered particle. The dominant Higgs boson production mechanism within the SM is the loop-induced gluon-fusion process  $gg \rightarrow H$  that is mediated by top and to a lesser extent bottom triangle loops as exemplified in Fig. 1. Although the total inclusive production rate agrees with the SM prediction within uncertainties, it is not clear that this production process is indeed loop-induced. For an experimental proof of the loop nature of the gluon-fusion process the top mass effects of the formfactors describing the Higgs coupling to gluons have to be measured. A point-like Higgs coupling to gluons is defined in terms of the effective Lagrangian

$$\mathcal{L}_{eff} = c_g \frac{\alpha_s}{\pi} G^{a\mu\nu} G_{\mu\nu}^a \frac{H}{v} \quad (1.1)$$

with  $\alpha_s$  denoting the strong coupling constant,  $G^{a\mu\nu}$  the gluon field strength tensor,  $H$  the Higgs field and  $v$  the electroweak vacuum expectation value. The Wilson coefficient  $c_g$  is adjusted to reproduce the measured inclusive cross section. In order to distinguish between a point-like Higgs coupling to gluons and the loop-induced type a large energy scale has to be inserted into the loop. At LO the gluon fusion process proceeds at the fixed scale given by the Higgs mass. The first distribution that gives rise to a variable energy scale inside the loops is the transverse momentum distribution of the Higgs particle that is generated primarily by the additional radiation of a gluon at LO (see Fig. 2). The comparison of the

$p_T$  distribution at small and large values of  $p_T$  allows for a distinction between top mass effects due to the loop contributions and a top mass independent point-like Higgs coupling to gluons [4]. First studies of the prospects at the LHC to resolve the Higgs coupling to gluons have been made recently [5]. These studies, however, are all theory-based while a rigorous experimental study is missing so far. The purpose of this letter is to describe and present the results of our analysis of the  $p_T$  spectrum of the Higgs particle with a detailed inclusion of experimental effects. In this way our study goes significantly beyond those of Refs. [5].

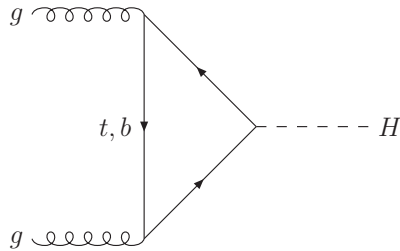


**Figure 1.** Gluon fusion  $gg \rightarrow H$  at leading order mediated by top and bottom triangle loops.

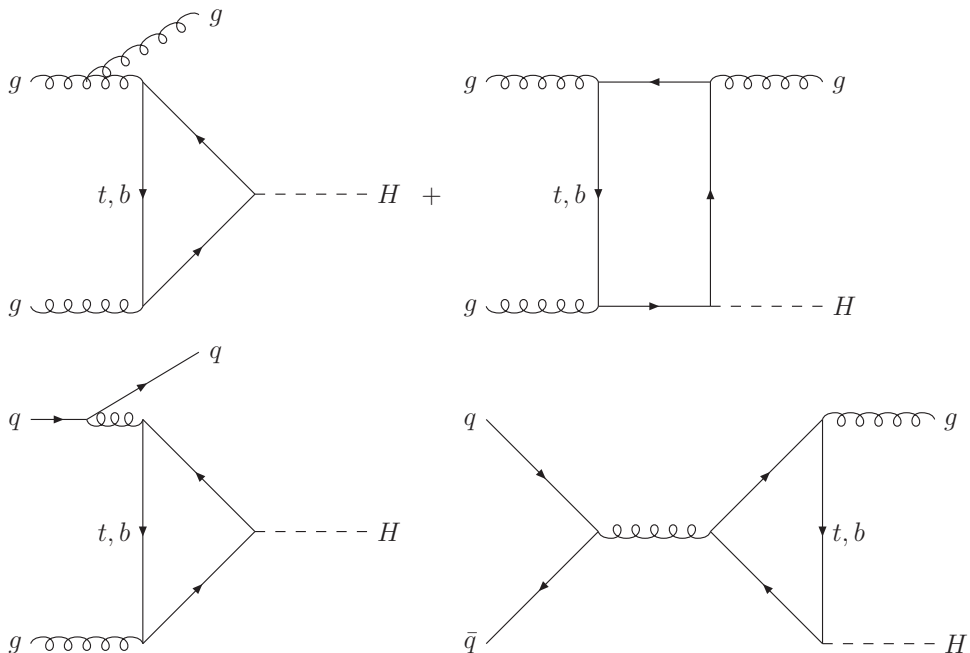


**Figure 2.** Generic diagrams for Higgs production in association with a jet via gluon fusion at leading order mediated by top and bottom triangle loops generated by  $gg, qq, q\bar{q}$  initial states.

The NLO corrections to the  $p_T$ -distribution are only known in the limit of a heavy

top quark [6] supplemented by subleading terms in the inverse top mass at NLO [7]. As for the inclusive cross section the QCD corrections are large and positive. Recently the NNLO QCD corrections to the  $p_T$  distribution have been derived in the heavy top limit yielding a further moderate increase of  $\sim 30\%$  [8], thus corroborating a reliable perturbative behaviour.

Since the pure LO and NLO results diverge for  $p_T \rightarrow 0$ , the small  $p_T$  region requires a soft gluon resummation for a reliable prediction. This resummation has been performed systematically for the top quark loops in Ref. [9], neglecting finite top mass effects at NLO. Soft gluon effects factorize, so that the top mass effects at small  $p_T$  are well approximated by the LO mass dependence for small Higgs masses [10–12]. Since the top-loop contribution dominates the cross section for the SM Higgs boson, the only limiting factor of the NLO+NNLL result as implemented in HqT or HRes [13] is thus the heavy-top approximation of the NLO corrections which affects the whole  $p_T$  range for large Higgs masses and the large  $p_T$  region in particular for all Higgs masses. It has been shown that the subleading NLO terms in the inverse top mass affect the  $p_T$  distribution by less than 10% for  $p_T \lesssim 300$  GeV, if the full LO mass dependence is taken into account [7].

In addition to the leading top-quark contribution the bottom quark loops amount to about  $-6\%$  in the inclusive cross section [14]. However, at leading order the bottom quark contribution is only sizable for small  $p_T$ , while for larger  $p_T$  values it can safely be neglected. Recently, bottom quark contributions have been included in the predictions for the resummed  $p_T$ -distributions [10–12, 15–18]. However, soft-gluon-resummation and bottom-quark effects do not play a role in our analysis that just concentrates on the shape at large  $p_T$  values, where the resummed predictions coincide with the fixed-order results.

## 2 Simulation setup

The focus of this study is on Higgs boson decays to two photons, as this final state provides a reasonably large signal-to-background ( $S/B$ ) ratio combined with a fair Higgs boson transverse momentum ( $p_\perp$ ) resolution. The alternative decay  $H \rightarrow ZZ^{(*)} \rightarrow 4\ell$  ( $\ell = e, \mu$ ) would offer superior  $S/B$  and  $p_\perp$  resolution, but suffers from even smaller statistics due to the very small effective branching fraction. Signal (background) event samples corresponding to proton-proton collisions at  $\sqrt{s} = 14$  TeV are produced with NLO (LO) event generators. Subsequently these data are passed through a parametrized detector simulation.

The signal events  $H \rightarrow \gamma\gamma$  are generated with MC@NLO 4.10 [19, 20] with a dynamic scale of  $\mu = \frac{1}{2} \sqrt{m_H^2 + p_\perp^2}$ , where  $m_H = 125$  GeV is the Higgs boson mass. For the loop-induced process, the exact top and bottom quark mass dependence is taken into account following the two-step procedure advocated in Ref. [15]. The events are hadronized with Herwig++ [21] using the cluster model of [22]; the shower evolution is performed with the algorithm described in [23]. For systematic studies, the QCD renormalization  $\mu_R$  and factorization  $\mu_F$  scales are varied according to the recipe provided in [24], i.e., from 0.5 to 2.0 times the nominal value  $\mu$ , excluding  $\mu_R/\mu_F = 1/4$  and 4. This variation not only changes the total production cross section, but also affects the shape of the Higgs boson

high- $p_{\perp}$  distribution. The MSTW08 [25] set of parton distribution functions (PDF) is used as default, while for systematic studies, NNPDF 2.3 [26] and CT10 [27] are considered. The total gluon fusion cross section for Higgs boson production is normalized to  $\sigma = 49.5$  pb with the uncertainties mentioned in Ref. [24]. Eventually, the total gluon fusion cross section will be measured with a substantially better experimental precision. The branching fraction for the considered final state is  $\mathcal{B}(H \rightarrow \gamma\gamma) = 2.28 \times 10^{-3}$ , with a relative uncertainty of 5% [28] which has been obtained from combining results of `Hdecay` [29] and `Prophecy4f` [30].

Using `Powheg` [31] to simulate the two signal Higgs boson scenarios instead of `MC@NLO` does not change the conclusion of this paper in a significant way.

The diphoton background events are generated with `Sherpa` V1.4.0 [32] with leading-order MSTW08 PDFs. In addition to the two photons, one or two jets are allowed in the process. Three requirements are applied at the generator level: (1) the generated photon energy is required to be  $E > 30$  GeV, (2) the invariant mass of the two photons must be in the range  $50 < m_{\gamma\gamma} < 200$  GeV and (3) the diphoton  $p_{\perp}$  has to fulfill  $p_{\perp} > 130$  GeV. In this kinematic region, the total cross section determined by `Sherpa` is  $\sigma_{\text{tot}} = 1.6$  pb. We assume an uncertainty of 40% on this cross section in the high- $p_{\perp}$  region.

The diphoton  $p_{\perp}$  distribution has been measured by ATLAS and CMS in  $pp$  collisions at  $\sqrt{s} = 7$  TeV. ATLAS showed in Ref. [33] that for  $p_{\perp} > 300$  GeV the diphoton sample is dominated by two real photons and that contributions from one or two jets misidentified as photons are roughly at the 10% level. The high- $p_{\perp}$  data are very well described in shape by the `Sherpa` (and `Pythia`) MC simulations. For the rate, the ATLAS collaboration scaled the expectations of `Sherpa` 1.3.1 up by 20%. The CMS collaboration [34] found very good agreement of `Sherpa` 1.4.0 (the same version is used for the present analysis) with the differential and integrated diphoton cross sections, albeit restricted to somewhat lower diphoton  $p_{\perp}$ .

The detector response simulation is based on `Delphes` 3 [35]. The default card for the CMS detector, included in the `Delphes` 3 distribution, is used. One modification is applied to the card: the cone for the calculation of photon isolation is reduced from  $\Delta R = \sqrt{\Delta\eta^2 + \Delta\phi^2} = 0.5$  to  $\Delta R = 0.1$ . The original setting leads to a noticeable inefficiency for Higgs bosons measurements at very large  $p_{\perp}$ , as the two photons are reconstructed close to each other. The performance of the ATLAS detector would likely be comparable, given the very similar performance of CMS and ATLAS in the Higgs boson measurements to date.

A significant limitation at the high-luminosity LHC (HL-LHC) will be the pile-up, currently estimated at around 140 overlapping events per bunch crossing. At present there is no complete understanding on the exact details of photon measurement and identification performance for that LHC and detector configuration. The current ‘particle-flow’ approach (also implemented in `Delphes` 3) is likely to be replaced by more powerful algorithms, which will allow for much better mitigation of pile-up effects than the present photon reconstruction. For the time being, we do not include pile-up in the detector simulation and account for this with a large selection efficiency uncertainty. It should be stressed that in this analysis no jet information is used, the only ingredients are high- $p_{\perp}$  photons.

We assume furthermore that events with  $H \rightarrow \gamma\gamma$  candidates at high  $p_{\perp}$  can be triggered with a negligible inefficiency.

### 3 Analysis

The purpose of this analysis is an estimate of the expected sensitivity to discriminate between the loop-induced and a point-like Higgs boson coupling. For this purpose, Higgs boson samples corresponding to the two hypotheses combined with diphoton background samples are studied. The invariant mass distribution provides the primary means to separate the Higgs boson signal from the diphoton background. As the expected number of Higgs bosons in the high- $p_{\perp}$  region differs between the two hypotheses, the invariant mass distribution also provides a powerful handle to distinguish between the two hypotheses. In addition the  $p_{\perp}$  distribution, where the two hypotheses lead to different shapes, provides additional separation power as illustrated in Fig. 3 (left).

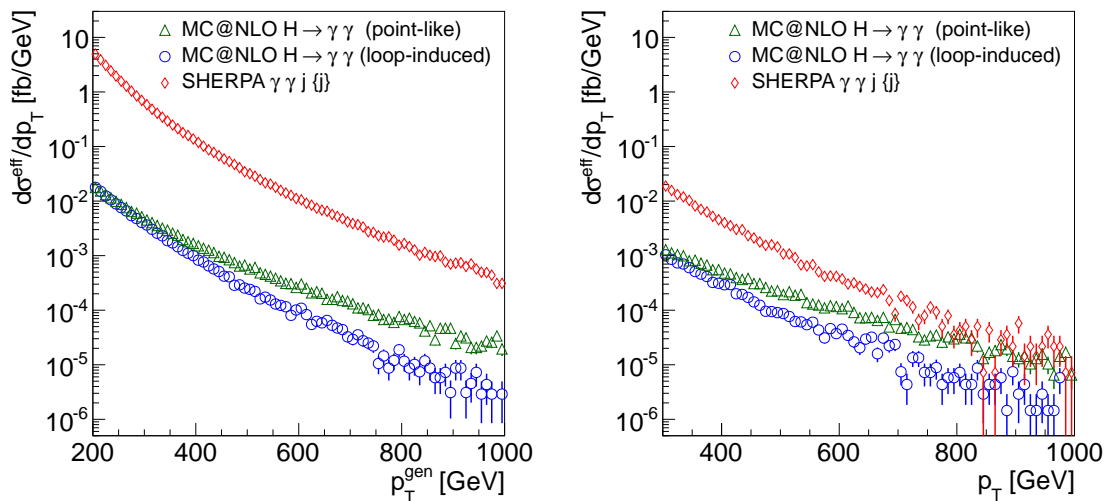


**Figure 3.** Differential production cross section as generated (left) and reconstructed after all analysis requirements (right). The effective cross section includes  $\mathcal{B}(H \rightarrow \gamma\gamma)$  for the Higgs boson cross sections (left and right), and the analysis efficiency for all cross sections (right). The error bars show the statistical uncertainty only.

The data analysis uses reconstructed objects from the `Delphes 3` detector simulation. No attempt is made to unfold the true Higgs boson  $p_{\perp}$  spectrum from the ‘reconstructed’ spectrum. Rather the ‘reconstructed’  $p_{\perp}$ -spectra from Higgs boson signal hypotheses and diphoton background are used to fit the combined ‘data’ spectra.

#### 3.1 Event Reconstruction

Reconstructed and identified photons from `Delphes 3` are subject to additional requirements. The isolation requirement of each photon is further tightened: the maximum energy flow in the form of tracks or energy clusters (except for the other photon forming the Higgs boson candidate) allowed within a cone of  $\Delta R < 0.3$  around the photon momentum is required to have  $p_{\perp} < 0.5$  GeV. The efficiency of this requirement is 52% for signal events and 17% for background events, nearly independent of the diphoton  $p_{\perp}$  requirement.

This requirement is quite strict, but not inconsistent with present capabilities [36] using area-based energy subtraction procedures [37]. As mentioned above, an improved pileup treatment will be required for the successful usage of the photon isolation variable at the HL-LHC.

The two photons with the largest  $p_{\perp}$  are combined to form Higgs boson candidates. The diphoton invariant mass must fulfill  $70 < m_{\gamma\gamma} < 180$  GeV. The leading (subleading) photon has to fulfill  $E_T > 80(50)$  GeV and for both photons  $|\eta| < 2.5$  is required. No jet information is used in this analysis, even though implicitly there will be jets as we require for the diphoton  $p_{\perp} > 300$  GeV (this will be referred to as high- $p_{\perp}$  region). For this kinematic region the signal (background) selection efficiency is 32.3% (3.4%). The values for the single and diphoton  $p_{\perp}$  requirements were optimized by maximizing the expected hypothesis discrimination sensitivity.

In Fig. 3 (right) the effective differential cross section for signal and background after the event selection is shown. The background contribution is found to be very large even after the above selection. The average expected diphoton invariant mass and  $p_{\perp}$  distributions for an integrated luminosity of  $1000 \text{ fb}^{-1}$  are shown in Fig. 4, where signal and background have been combined (in contrast to Fig. 3, where signal and background are shown separately). The Higgs boson invariant mass resolution depends strongly on the diphoton  $p_{\perp}$  and is limited by the angular resolution in the kinematic range of this analysis.

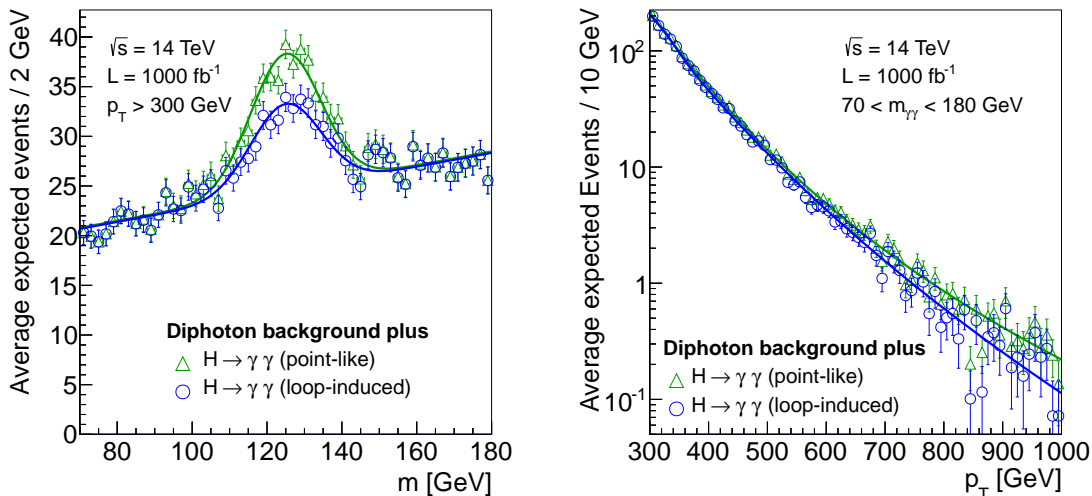


**Figure 4.** Average expected event yields vs diphoton invariant mass (left) and diphoton  $p_{\perp}$  (right), normalized to  $1000 \text{ fb}^{-1}$ . The histograms contain the background plus the point-like Higgs production (open triangles) and the background plus the loop-induced Higgs production (open circles). The background component is identical for both hypotheses. The error bars show the statistical uncertainty only.

The invariant mass distribution for the signal is well described by a single Gaussian with standard deviation  $\sigma = 9.4 \text{ GeV}$  in the high- $p_{\perp}$  region. The background is parametrized

with a first degree polynomial. The rising background invariant mass shape arises from the selection criteria applied, in particular the very high- $p_{\perp}$  requirement and the photon isolation criteria. In the high- $p_{\perp}$  region, the shape of the signal and background  $p_{\perp}$  distributions can be described with a log normal distribution. The free parameters of the fit are: the Higgs boson yield, the background yield, two parameters ( $\mu$  and  $k$ ) each for the signal and background log normal distributions, and the slope of the polynomial describing the background mass distribution. The position and width of the Higgs boson peak are fixed.

### 3.2 Sensitivity Analysis

The sensitivity study is based on a two-dimensional extended unbinned maximum likelihood fit to the diphoton invariant mass and  $p_{\perp}$  distributions using the probability density functions described above. The  $H_0$  hypothesis corresponds to the scenario of loop-induced Higgs boson production plus the diphoton background. The  $H_1$  hypothesis describes the point-like Higgs boson production together with the diphoton background.

Toy data are generated for the two hypotheses, where the event numbers in the toy datasets depend on the integrated luminosity studied. In Fig. 5 an example toy data set is shown. In the high- $p_{\perp}$  region and for a luminosity of  $\mathcal{L} = 1000 \text{ fb}^{-1}$  the expected background yield is  $N_B = 1360$ , while the signal components for the respective hypotheses are  $N_S^{H_0} = 86$  and  $N_S^{H_1} = 150$  (see below for a discussion of the systematic uncertainties). From the negative log-likelihood ratio for the two hypotheses, a test statistic  $q = -2 \ln(\mathcal{L}_{H_1}/\mathcal{L}_{H_0})$  is constructed. The background parameters (normalization and the shape of the mass distribution and the shape of the  $p_{\perp}$  distribution) are treated as nuisance parameters and profiled over. The expected separation between  $H_0$  and  $H_1$  is quantified as follows [38–40]: We determine a midpoint  $\tilde{q}$  between the medians of the two test statistic distributions such that  $\mathcal{P}(q \geq \tilde{q}|H_1) = \mathcal{P}(q \leq \tilde{q}|H_0)$ . This tail probability is converted into a significance  $\tilde{Z}$  using the one-sided Gaussian tail convention. For the separation power we quote  $Z = 2\tilde{Z}$ , as the midpoint  $\tilde{q}$  is half-way between the medians of the two test statistic distributions. Using 10 000 toy data sets a relative sensitivity uncertainty of about 1% is achieved. To study systematic uncertainties, different toy data sets are generated corresponding to the uncertainty under study.

## 4 Results

In Fig. 6 the result of the sensitivity study is shown. The central expectation corresponds to the expected signal and background numbers as discussed above. Systematic uncertainties on the expected sensitivity arise from various sources.

Experimental uncertainties have a significant impact as this sensitivity study ventures into a pile-up regime where adequate algorithms are still to be developed. For the signal efficiency we assume a relative uncertainty of  $\pm 20\%$ . As no diphoton measurement exists for the kinematic range considered in this analysis, and since no jet to photon misidentification is considered, an uncertainty of  $\pm 40\%$  is used for the background yield. The sampling uncertainty from the limited statistics in the toy data sets is minor for the sensitivity regime found here.

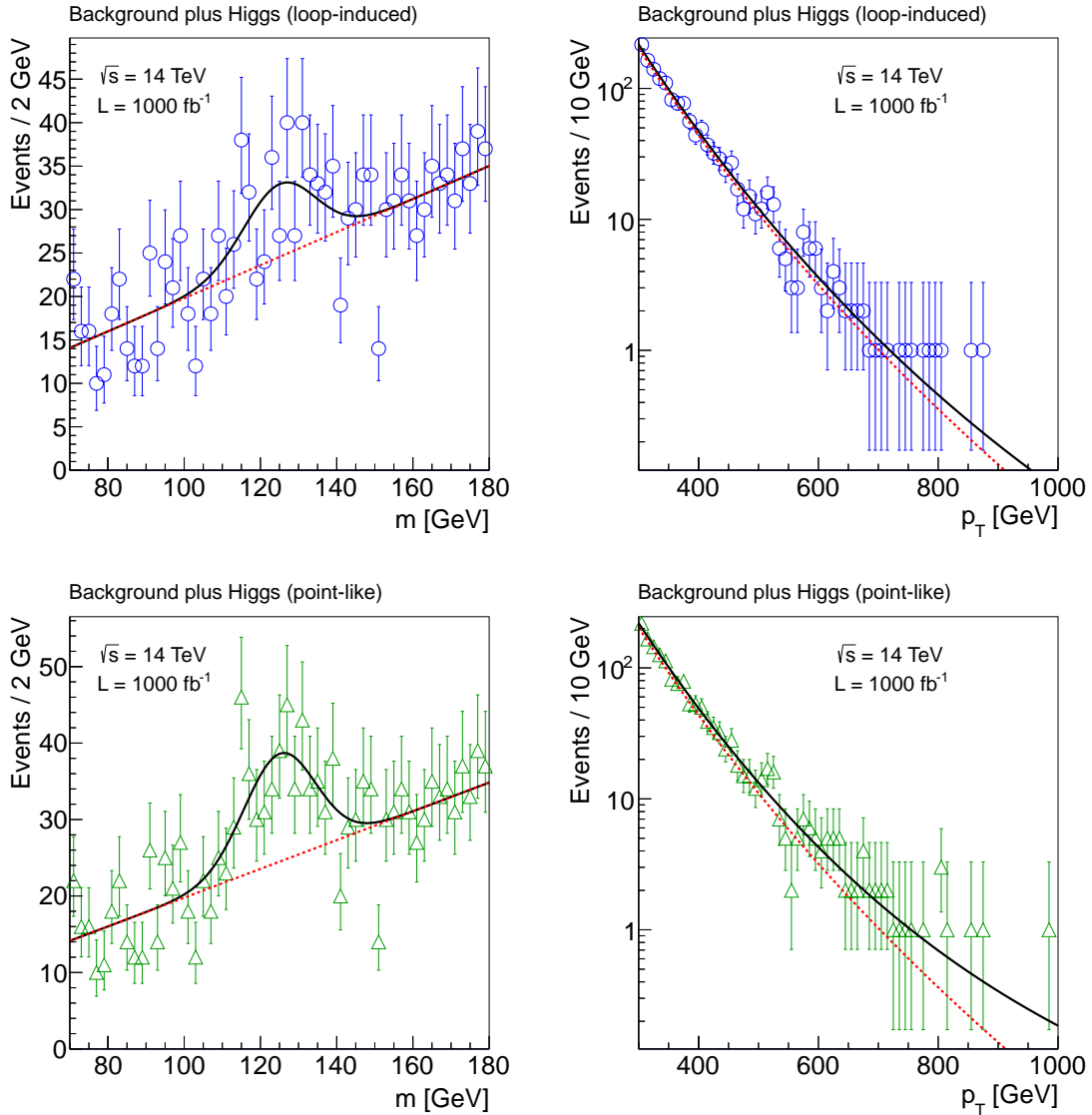


**Figure 5.** Example toy data set with overlaid projections of the extended unbinned maximum likelihood fits for the diphoton invariant mass (left) and the diphoton  $p_{\perp}$  (right). The  $H_0$  hypothesis (loop-induced Higgs boson production) is shown in the top row, the  $H_1$  hypothesis (point-like Higgs boson production) is shown in the bottom row. The background component is identical for both hypotheses. The (black) solid curves shows the signal+background fit, the (red) dashed line shows the background component. The error bars show the statistical uncertainty only.

Theoretical uncertainties have a larger impact on the expected sensitivity. The scale uncertainties from  $\mu_R$  and  $\mu_F$  affect both the event yields for the two hypothesis and (to a smaller extent) the shape of the  $p_{\perp}$  distributions. The missing top mass effects are parametrized with

$$\frac{\Delta x}{x} = \left( \frac{p_{\perp} - 40 \text{ GeV}}{100 \text{ GeV}} \right)^2 \times 1.5\%,$$

where  $x = d\sigma/dp_{\perp}$ . This parametrization has been adjusted to the known systematic top mass effects obtained in Ref. [7]. Uncertainties from a variation of the PDFs or the top quark mass are found to be negligible.

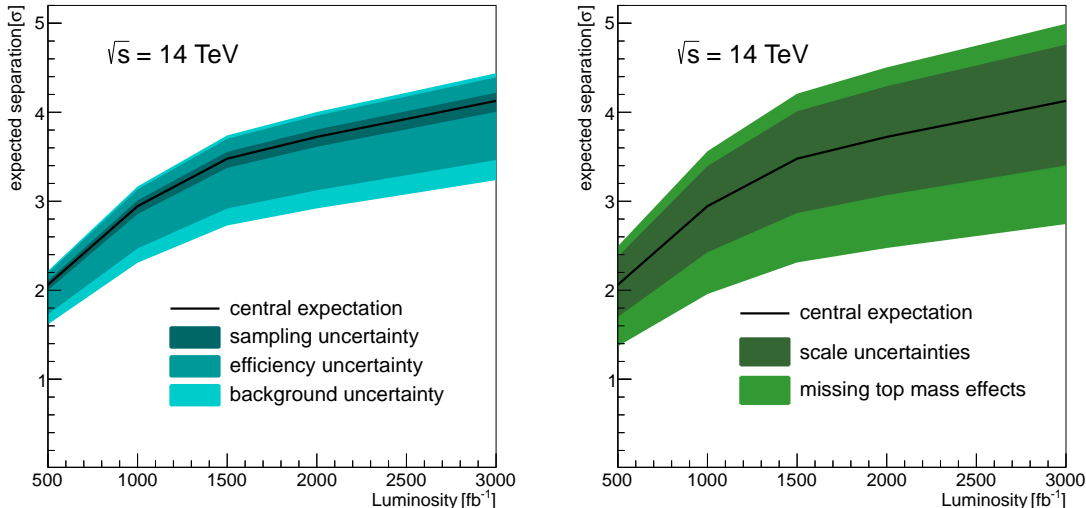


**Figure 6.** Expected sensitivity vs. integrated luminosity. The experimental uncertainties (left) are combined quadratically, the theoretical uncertainties (right) are added linearly.

The two Higgs boson hypotheses can be separated with 2 standard deviations ( $\sigma$ ) with an integrated luminosity of about  $500 \text{ fb}^{-1}$ . With a luminosity of  $1000 \text{ fb}^{-1}$  the expected separation sensitivity is about  $3\sigma$ . The largest experimental uncertainty (downwards) arises from the background uncertainty in the high- $p_{\perp}$  region. A combination with other Higgs boson final states and a more elaborate analysis would help to improve the sensitivity. However, theoretical uncertainties and missing top mass effects also have a large impact on the sensitivity as can be inferred from Fig. 6 (right panel). A reduction requires the full implementation of higher-order effects on the transverse-momentum distribution in the generators and in particular the full top mass effects at NLO that have not been calculated so far.

## 5 Conclusions

We have studied the possibility to separate in gluon fusion loop-induced Higgs boson production from point-like production. Using the Higgs boson yields (normalized to the overall rate) and the shape of the Higgs boson  $p_{\perp}$  distribution the two hypotheses can be separated with  $2\sigma$  with an integrated luminosity of about  $500 \text{ fb}^{-1}$  (likely after Run-2 of the LHC). The largest systematic uncertainty affecting this estimate is the background event yield, as that strongly dilutes the difference between the two Higgs boson hypotheses. Understanding and mitigating the impact from pile up will be crucial for this analysis.

## 6 Acknowledgements

We are grateful to S. Frixione for his help with `MC@NLO` and to A. Vicini for his help with `Powheg`. We thank our CMS colleagues, in particular M. Donega, for useful discussions.

## References

- [1] G. Aad *et al.* [ATLAS Collaboration], Phys. Lett. **B716** (2012) 1; S. Chatrchyan *et al.* [CMS Collaboration], Phys. Lett. **B716** (2012) 30.
- [2] [CMS Collaboration], CMS-PAS-HIG-13-005; [ATLAS Collaboration], ATLAS-CONF-2013-034.
- [3] P.W. Higgs, Phys. Lett. **12** (1964) 132; Phys. Rev. Lett. **13** (1964) 508 and Phys. Rev. **145** (1964) 1156; F. Inlet and R. Brout, Phys. Rev. Lett. **13** (1964) 321; G.S. Guralnik, C.R. Hagen and T.W. Kibble, Phys. Rev. Lett. **13** (1964) 585.
- [4] R. K. Ellis, I. Hinchliffe, M. Soldate and J. J. van der Bij, Nucl. Phys. B **297** (1988) 221; U. Baur and E. W. N. Glover, Nucl. Phys. B **339** (1990) 38; O. Brein and W. Hollik, Phys. Rev. D **68** (2003) 095006; U. Langenegger, M. Spira, A. Starodumov and P. Trub, JHEP **0606** (2006) 035; O. Brein and W. Hollik, Phys. Rev. D **76** (2007) 035002.
- [5] R. V. Harlander and T. Neumann, Phys. Rev. D **88** (2013) 074015; A. Banfi, A. Martin and V. Sanz, JHEP **1408** (2014) 053; A. Azatov and A. Paul, JHEP **1401** (2014) 014; C. Englert, M. McCullough and M. Spannowsky, Phys. Rev. D **89** (2014) 013013; C. Grojean, E. Salvioni, M. Schlaffer and A. Weiler, JHEP **1405** (2014) 022; M. Schlaffer, M. Spannowsky, M. Takeuchi, A. Weiler and C. Wymant, Eur. Phys. J. C **74** (2014) 10, 3120. M. Buschmann, C. Englert, D. Goncalves, T. Plehn and M. Spannowsky, Phys. Rev. D **90** (2014) 1, 013010; M. Buschmann, D. Goncalves, S. Kuttimalai, M. Schonherr, F. Krauss and T. Plehn, JHEP **1502** (2015) 038.
- [6] C. R. Schmidt, Phys. Lett. B **413** (1997) 391; D. de Florian, M. Grazzini and Z. Kunszt, Phys. Rev. Lett. **82** (1999) 5209; V. Ravindran, J. Smith and W. L. Van Neerven, Nucl. Phys. B **634** (2002) 247; C. J. Glosser and C. R. Schmidt, JHEP **0212** (2002) 016; C. Anastasiou, K. Melnikov and F. Petriello, Phys. Rev. Lett. **93** (2004) 262002 and Nucl. Phys. B **724** (2005) 197; S. Dawson, I. M. Lewis and M. Zeng, Phys. Rev. D **90** (2014) 9, 093007; K. Hamilton, P. Nason and G. Zanderighi, arXiv:1501.04637 [hep-ph].
- [7] R.V. Harlander, T. Neumann, K.J. Ozeren and M. Wiesemann, JHEP **1208** (2012) 139.
- [8] T. Gehrmann, M. Jaquier, E. W. N. Glover and A. Koukoutsakis, JHEP **1202** (2012) 056; R. Boughezal, F. Caola, K. Melnikov, F. Petriello and M. Schulze, JHEP **1306** (2013) 072; X. Chen, T. Gehrmann, E. W. N. Glover and M. Jaquier, Phys. Lett. B **740** (2015) 147; R. Boughezal, F. Caola, K. Melnikov, F. Petriello and M. Schulze, arXiv:1504.07922 [hep-ph]; R. Boughezal, C. Focke, W. Giele, X. Liu and F. Petriello, Phys. Lett. B **748** (2015) 5.
- [9] S. Catani, E. D’Emilio and L. Trentadue, Phys. Lett. B **211** (1988) 335; I. Hinchliffe and S.F. Novaes, Phys. Rev. D **38** (1988) 3475; R. P. Kauffman, Phys. Rev. D **44** (1991) 1415 and Phys. Rev. D **45** (1992) 1512; C. Balazs and C.P. Yuan, Phys. Lett. B **478** (2000) 192; E. L. Berger and J.W. Qiu, Phys. Rev. D **67** (2003) 034026; A. Kulesza and W. J. Stirling, JHEP **0312** (2003) 056; A. Kulesza, G. Sterman and W. Vogelsang, Phys. Rev. D **69** (2004) 014012; A. Gawron and J. Kwiecinski, Phys. Rev. D **70** (2004) 014003; G. Watt, A. D. Martin and M. G. Ryskin, Phys. Rev. D **70** (2004) 014012 [Erratum-ibid. D **70** (2004)

- 079902]; A. V. Lipatov and N. P. Zotov, *Eur. Phys. J. C* **44** (2005) 559; D. de Florian and M. Grazzini, *Phys. Rev. Lett.* **85** (2000) 4678; *Nucl. Phys. B* **616** (2001) 247; S. Catani, D. de Florian and M. Grazzini, *Nucl. Phys. B* **596** (2001) 299; G. Bozzi, S. Catani, D. de Florian and M. Grazzini, *Phys. Lett. B* **564** (2003) 65; G. Bozzi, S. Catani, D. de Florian and M. Grazzini, *Nucl. Phys. B* **737** (2006) 73 and *Nucl. Phys. B* **791** (2008) 1; D. de Florian, G. Ferrera, M. Grazzini and D. Tommasini, *JHEP* **1111** (2011) 064; D. Neill, I. Z. Rothstein and V. Vaidya, arXiv:1503.00005 [hep-ph].
- [10] J. Alwall, Q. Li and F. Maltoni, *Phys. Rev. D* **85** (2012) 014031.
- [11] E. Bagnaschi, G. Degrossi, P. Slavich and A. Vicini, *JHEP* **1202** (2012) 088.
- [12] H. Mantler and M. Wiesemann, *Eur. Phys. J. C* **73** (2013) 6, 2467.
- [13] <http://theory.fi.infn.it/grazzini/codes.html>
- [14] D. Graudenz, M. Spira and P. M. Zerwas, *Phys. Rev. Lett.* **70** (1993) 1372; M. Spira, A. Djouadi, D. Graudenz and P. M. Zerwas, *Nucl. Phys. B* **453** (1995) 17; R. Harlander and P. Kant, *JHEP* **0512** (2005) 015.
- [15] M. Grazzini and H. Sargsyan, *JHEP* **1309** (2013) 129.
- [16] A. Banfi, P. F. Monni and G. Zanderighi, *JHEP* **1401** (2014) 097;
- [17] R. V. Harlander, H. Mantler and M. Wiesemann, *JHEP* **1411** (2014) 116;
- [18] E. Bagnaschi and A. Vicini, arXiv:1505.00735 [hep-ph].
- [19] S. Frixione and B. R. Webber, *JHEP* **0206** (2002) 029, [[hep-ph/0204244](http://arxiv.org/abs/hep-ph/0204244)].
- [20] <http://www.hep.phy.cam.ac.uk/theory/webber/MCatNLO>
- [21] M. Bahr *et al.*, *Eur. Phys. J. C* **58** (2008) 639.
- [22] B. R. Webber, *Nucl. Phys. B* **238**, 492 (1984).
- [23] G. Marchesini and B. R. Webber, *Nucl. Phys. B* **238**, 1 (1984); G. Marchesini and B. R. Webber, *Nucl. Phys. B* **310**, 461 (1988); S. Gieseke, P. Stephens and B. Webber, *JHEP* **0312**, 045 (2003).
- [24] S. Dittmaier *et al.* [LHC Higgs Cross Section Working Group Collaboration], arXiv:1101.0593 [hep-ph]; updated at <https://twiki.cern.ch/twiki/bin/view/LHCPhysics/LHCHXSWGGSF>.
- [25] A. D. Martin, W. J. Stirling, R. S. Thorne and G. Watt, *Eur. Phys. J. C* **63**, 189 (2009).
- [26] R. D. Ball, V. Bertone, S. Carrazza, C. S. Deans, L. Del Debbio, S. Forte, A. Guffanti and N. P. Hartland *et al.*, *Nucl. Phys. B* **867**, 244 (2013).
- [27] H. L. Lai, M. Guzzi, J. Huston, Z. Li, P. M. Nadolsky, J. Pumplin and C.-P. Yuan, *Phys. Rev. D* **82**, 074024 (2010).
- [28] A. Denner, S. Heinemeyer, I. Puljak, D. Rebuszi and M. Spira, *Eur. Phys. J. C* **71** (2011) 1753.
- [29] A. Djouadi, J. Kalinowski and M. Spira, *Comput. Phys. Commun.* **108** (1998) 56; A. Djouadi, M. M. Mühlleitner and M. Spira, *Acta Phys. Polon. B* **38** (2007) 635.
- [30] A. Bredenstein, A. Denner, S. Dittmaier and M. M. Weber, *Phys. Rev. D* **74** (2006) 013004 and *JHEP* **0702** (2007) 080.

- [31] P. Nason, JHEP **0411**, 040 (2004) [hep-ph/0409146]; S. Frixione, P. Nason and C. Oleari, JHEP **0711**, 070 (2007); S. Alioli, P. Nason, C. Oleari and E. Re, JHEP **1006**, 043 (2010); E. Bagnaschi, G. Degrossi, P. Slavich and A. Vicini, JHEP **1202**, 088 (2012).
- [32] T. Gleisberg, S. Hoeche, F. Krauss, M. Schonherr, S. Schumann, F. Siegert and J. Winter, JHEP **0902**, 007 (2009); S. Schumann and F. Krauss, JHEP **0803**, 038 (2008); F. Krauss, R. Kuhn and G. Soff, JHEP **0202**, 044 (2002) [hep-ph/0109036]; T. Gleisberg and S. Hoeche, JHEP **0812**, 039 (2008); S. Hoeche, F. Krauss, S. Schumann and F. Siegert, JHEP **0905**, 053 (2009); M. Schonherr and F. Krauss, JHEP **0812**, 018 (2008).
- [33] G. Aad *et al.* [ATLAS Collaboration], JHEP **1301**, 086 (2013).
- [34] S. Chatrchyan *et al.* [CMS Collaboration], Eur. Phys. J. C **74**, no. 11, 3129 (2014).
- [35] J. de Favereau *et al.* [DELPHES 3 Collaboration], JHEP **1402**, 057 (2014).
- [36] V. Chachatryan *et al.* [CMS Collaboration], arXiv:1502.02702 [physics.ins-det].
- [37] M. Cacciari and G. P. Salam, Phys. Lett. B **659**, 119 (2008).
- [38] R. Cousins, J. Mumford, J. Tucker and V. Valuev, JHEP **0511**, 046 (2005).
- [39] Y. Gao, A. V. Gritsan, Z. Guo, K. Melnikov, M. Schulze and N. V. Tran, Phys. Rev. D **81**, 075022 (2010).
- [40] M. Chen, T. Cheng, J. S. Gainer, A. Korytov, K. T. Matchev, P. Milenovic, G. Mitselmakher and M. Park *et al.*, Phys. Rev. D **89**, 034002 (2014).